Chemistry of Polydentate Ligands. Part 8.[1] Preparation and Properties of Iron(II) Complexes with Quinquedentate Macrocyclic Ligands. Crystal and Molecular Structure of a Compound where High-spin Fe^{II} sits in the Ligand Cavity. Electrochemistry of a Series of Complexes with the Macrocycles

By **Michael M. Bishop, Jack Lewis,* Timothy D. O'Donoghue, Paul R. Raithby, and John N. Ramsden,** University Chemical Laboratory, Lensfield Road, Cambridge CB2 1EW

Complexes of quinquedentate macrocyclic ligands with Fe^{II} have been prepared by condensation of 2,6-diacetylpyridine and 2,6-diformylpyridine with 2,9-di(1-methylhydrazino)-1,10-phenanthroline monohydrochloride in the presence of iron(II) templates. Magnetic susceptibility measurements and Mössbauer parameters show that the complexes are high spin, while chemical evidence indicates that the macrocycles encompass iron(II). This is confirmed by a structure determination on a single crystal of $[FeC_{23}H_{25}N_7O_2][B_2F_8]$, which is monoclinic with $a = 14.152(3)$, $b = 11.464(11)$, $c = 16.732(5)$ Å, $\beta = 93.56(3)°$, $Z = 4$, space group $P2_1/c$. Metal–donor nitrogen distances are 2.100(9), 2.112(8), 2.116(7), 2.242(8), and 2.276(8) Å. The co-ordination geometry of the iron(II) is pentagonal bipyramidal with water molecules occupying the axial sites: Fe–O distances are 2.213(7) and 2.194(7) Å. This structure is compared with those of high-spin iron(II) complexes of other macrocycles. Cyclic voltammetry data for selected complexes of Mn^{II}, Fe^{II}, Zn^{II}, and Cd^{II} with the ligands are presented: one-electron reductions produce π-anion radicals.

RECENT papers in this series have described the formation of complexes of Zn^{II}, Cd^{II}, Hg^{II}, and Mn^{II} with the quinquedentate ligands L^2 and L^3.[1,2] The complexes have pentagonal-pyramidal co-ordination geometry about the central ion, with the cation sitting above the plane of the macrocycle. The cations are essential for directing the ring closure. Only certain transition-metal ions have been found to be suitable for this template activity and, with the exception of high-spin Fe^{II}, the list is limited, for the penta-aza macrocycles, to cations having symmetric d^5 or d^{10} outer-electron configurations.[3–7] We report the extension of our investigations to the template synthesis of iron(II) complexes of the ligands L^2 and L^3. These compounds were considered to be candidates for exhibiting a dependence of co-ordination geometry on spin state, as is found with iron(II) porphyrins where high-spin Fe^{II} sits above the porphyrin plane[8] but intermediate or low-spin Fe^{II} is seated in the ligand plane.[8,9] In fact, the crystal structure of the iron(II) complex with L^3 shows that the high-spin metal ion sits within the ligand cavity.[10] Electrochemical data for complexes with the macrocycles are also disclosed.

RESULTS AND DISCUSSION

Iron(II) complexes of L^2 and L^3 were prepared by condensing 2,9-di(1-methylhydrazino)-1,10-phenanthroline, L^1·HCl, with 2,6-diformylpyridine and 2,6-diacetylpyridine respectively, in the presence of fresh $FeCl_2 \cdot 4H_2O$ as the template. Solvents were thoroughly deoxygenated beforehand and the reaction mixtures were refluxed under a stream of nitrogen. Dilute HCl, as a catalyst, hastens ring closure but is not essential to the reactions. The olive-green solids produced are stable in the atmosphere for a few days, but solutions are more sensitive to oxygen. Analytical data for the complexes are given in Table 1. Examining this information reveals a major difference between the iron(II) complexes of L^2 and L^3 and those containing Mn^{II}, Zn^{II}, and Cd^{II}; a chloride ion is not retained on precipitation of solids by addition of large anions to the iron(II) compounds.[1,2] The binding of a chloride ligand in $[M(L)Cl]^+$ ($M = Mn^{II}$, Zn^{II}, or Cd^{II}; $L = L^2$ or L^3) is taken as chemical evidence of

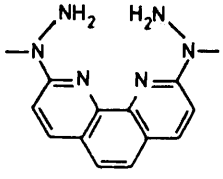

L^1

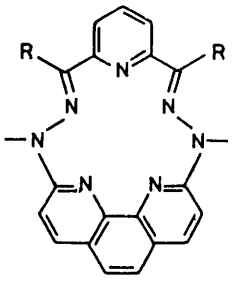

L^2: R = H
L^3: R = Me

differentiation between the two axial sites, which in turn is the result of the metal ions being too big to be encompassed within the plane of the macrocycles. By similar reasoning, the lack of retention of a chloride ion implies that the axial sites are equivalent in the iron(II) complexes and hence that the iron atoms sit in the macrocyclic planes. This conclusion is verified by the crystal structure of $[Fe(L^3)(OH_2)_2][BF_4]_2$, given below.

Further support for the equivalence of the axial environments is provided by the i.r. spectrum of $[Fe(L^3)(NCS)_2]$. The $\nu(C\equiv N)$ region contains a single band, at 2 060 cm^{-1}, indicative of co-ordination through the nitrogens.[5,11] Caution must be exercised in this assignment however, because accidental degeneracy, as with $[Mn(L^3)(NCS)_2]$, is an alternative explanation.[1] The lack of any N–H and carbonyl signals in the i.r. spectra does not distinguish between polymer formation and ring closure in the reactions, but the products are assigned as macrocycles after comparison with the spectrum of $[Fe(L^3)(OH_2)_2][BF_4]_2$, where the ligand is known to be a macrocycle.

Both the Mössbauer spectrum and the magnetic susceptibility of $[Fe(L^3)(OH_2)_2][BF_4]_2$ establish that the iron(II) is high spin: a quintet ground state. The room-temperature Mössbauer spectrum consists of a doublet, the parameters of which are a chemical shift of 1.01 mm s^{-1} relative to natural iron, and a quadrupole splitting of 2.74 mm s^{-1}. These values are characteristic of high-spin iron(II).[12] The magnetic moment of the complex was measured over the temperature range 93—295 K: the moment falls slightly with temperature but a plot of $1/\chi_m$, where χ_m is the effective molar magnetic susceptibility, against temperature gives a straight line. The Weiss constant is −32 K and the magnetic moment, measured from the gradient of the line, is 5.33 B.M.* Chemical, magnetic, and Mössbauer evidence therefore suggest that high-spin Fe^{II} sits in the plane of the ligand. This aspect was investigated further by growing crystals, dark green platelets, of one of the complexes and determining the crystal structure.

TABLE 1

Analytical data for iron(II) complexes with L^2 and L^3

Compound	Analysis (%) * C	H	N
$[Fe(L^2)(OH_2)_2][BF_4]_2$	39.3 (39.9)	3.3 (3.3)	15.6 (15.5)
$[Fe(L^3)(OH_2)_2][BF_4]_2$	42.3 (41.9)	3.7 (3.8)	14.8 (14.8)
$[Fe(L^3)(NCS)_2]$	53.0 (52.9)	3.8 (3.7)	22.4 (22.2)
$Fe(L^3)(OH_2)(PF_6)_2$	36.2 (36.4)	3.4 (3.1)	13.0 (12.9)

* Calculated values are given in parentheses.

Crystal and Molecular Structure Determination of $[Fe(L^3)(OH_2)_2][BF_4]_2$.—*Crystal data.* $C_{23}H_{25}B_2F_8FeN_7O_2$, $M = 660.97$, Monoclinic, $a = 14.153(3)$, $b = 11.464(11)$, $c = 16.732(5)$ Å, $\beta = 93.56(3)°$, $U = 2\,709.3$ Å^3; $D_c = 1.620$ g cm^{-3}, $Z = 4$, $\lambda = 0.710\,69$ Å, $\mu = 6.08$ cm^{-1}.

A crystal with dimensions *ca.* 0.42 × 0.385 × 0.063 mm was mounted under nitrogen in a Lindemann tube and used for data collection. The crystal was aligned about the *b* axis on a Stoe STADI-2 two-circle diffractometer, and cell parameters were obtained from zero-layer ω-angle and μ-angle measurements. Lorentz and polarisation effects were allowed for on the 5 319 recorded intensities (layers 0—*h*, 13, *l*) and a numerical

* Throughout this paper: 1 B.M. = 9.27 × 10^{-24} A m^2.

TABLE 2

Atom co-ordinates (× 10^4) with estimated standard deviations in parentheses

Atom	*x/a*	*y/b*	*z/c*
(*a*) Non-hydrogen atoms			
Fe(1)	7 493(1)	1 122(1)	1 183(1)
O(1)	8 818(5)	1 606(7)	1 875(4)
O(2)	6 181(5)	712(7)	471(4)
N(1)	8 247(6)	−56(8)	503(4)
N(2)	7 484(6)	−605(8)	1 811(4)
N(3)	7 034(6)	−661(8)	2 527(4)
N(4)	6 760(5)	1 270(7)	2 249(4)
N(5)	7 048(6)	2 879(7)	1 215(4)
N(6)	7 780(6)	3 260(8)	38(5)
N(7)	8 005(6)	2 111(8)	113(5)
C(1)	6 182(7)	541(10)	3 465(6)
C(2)	5 866(7)	1 628(10)	3 644(6)
C(3)	5 708(8)	3 738(11)	3 265(7)
C(4)	5 879(8)	4 622(12)	2 736(7)
C(5)	6 493(8)	5 185(11)	1 395(6)
C(6)	6 962(8)	4 837(10)	739(6)
C(7)	9 011(8)	−535(12)	−675(7)
C(8)	9 192(9)	−1 604(12)	−380(7)
C(9)	8 900(8)	−1 948(12)	346(6)
C(10)	8 419(7)	−1 120(11)	783(6)
C(11)	8 032(8)	−1 390(10)	1 570(6)
C(12)	6 641(7)	402(9)	2 739(5)
C(13)	6 430(7)	2 343(9)	2 422(5)
C(14)	6 599(7)	3 213(9)	1 859(5)
C(15)	7 263(7)	3 674(10)	680(6)
C(16)	8 331(7)	1 481(9)	−447(6)
C(17)	8 533(7)	272(10)	−219(6)
C(18)	5 983(7)	2 572(9)	3 138(6)
C(19)	6 317(7)	4 357(10)	2 000(6)
C(20)	8 415(9)	4 083(12)	−342(7)
C(21)	8 438(9)	1 857(12)	−1 303(6)
C(22)	8 383(9)	−2 483(11)	2 023(7)
C(23)	6 579(9)	−1 786(12)	2 734(7)
B(1)	4 019(10)	2 257(13)	241(8)
F(1)	3 999(6)	2 023(8)	−544(5)
F(2)	4 804(16)	2 755(20)	482(11)
F(2′)	4 575(14)	3 328(19)	315(11)
F(3)	3 195(6)	2 812(8)	425(5)
F(4)	3 799(14)	1 187(18)	539(10)
F(4′)	4 462(14)	1 613(18)	831(10)
B(2)	9 840(12)	4 643(16)	1 793(9)
F(5)	8 788(13)	4 573(19)	2 008(11)
F(5′)	9 119(15)	3 826(20)	1 722(11)
F(6)	9 544(14)	5 465(21)	1 143(11)
F(6′)	9 841(15)	5 576(22)	1 409(12)
F(7)	9 798(16)	3 601(17)	1 448(10)
F(7′)	10 642(14)	4 061(18)	1 537(10)
F(8)	10 254(14)	4 670(18)	2 540(12)
F(8′)	9 838(15)	5 048(18)	2 547(12)
(*b*) Hydrogen atoms			
H(1)	6 086(7)	−188(10)	3 861(6)
H(2)	5 517(7)	1 759(10)	4 193(6)
H(3)	5 350(8)	3 945(11)	3 799(7)
H(4)	5 686(8)	5 509(12)	2 869(7)
H(5)	6 262(8)	6 077(11)	1 450(6)
H(6)	7 097(8)	5 455(10)	272(6)
H(7)	9 233(8)	−297(12)	−1 259(7)
H(8)	9 580(9)	−2 212(12)	−727(7)
H(9)	9 035(8)	−2 818(12)	573(6)
H(201)	8 111(9)	4 946(12)	−343(7)
H(202)	8 505(9)	3 811(12)	−951(7)
H(203)	9 095(9)	4 093(12)	−11(7)
H(211)	8 729(9)	1 147(12)	−1 634(6)
H(212)	8 907(9)	2 600(12)	−1 311(6)
H(213)	7 753(9)	2 094(12)	−1 577(6)
H(221)	8 840(9)	−2 976(11)	1 655(7)
H(222)	7 785(9)	−3 014(11)	2 163(7)
H(223)	8 773(9)	−2 229(11)	2 571(7)
H(231)	6 261(9)	−1 699(12)	3 301(7)
H(232)	7 107(9)	−2 467(12)	2 776(7)
H(233)	6 039(9)	−2 006(12)	2 274(7)

absorption correction applied. Averaging equivalent reflections left 3 106 unique observed intensities with $I > 3\sigma(I)$, which were used in solving the structure. The fractional atomic co-ordinates of the Fe atom were

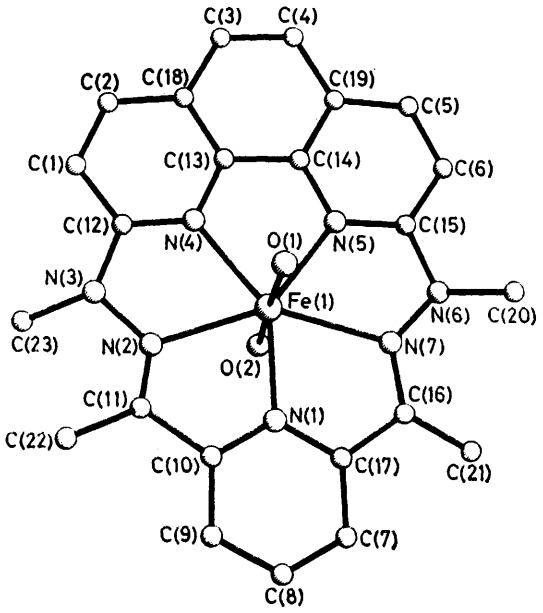

FIGURE 1 The molecular structure of $[Fe(L^3)(OH_2)_2]^{2+}$ and the atom-numbering scheme used. Hydrogen atoms have been omitted for clarity

derived from a Patterson synthesis and the lighter atoms were located in subsequent Fourier difference maps. The structure was refined using blocked full-matrix least-squares methods with anisotropic temperature factors for Fe and the N and O atoms, individual isotropic thermal parameters for C and B atoms, and common isotropic temperature factors for H(methyl), H(ring), and F atoms. Ring and methyl hydrogens were constrained to lie in geometrically idealised positions (C–H 1.08 Å), the methyl groups being treated as rigid groups pivoted about the carbons. Both BF_4^- anions are severely disordered. The final refinement coverged to $R' = \Sigma w^{\frac{1}{2}}(|F_o| - |F_c|)/\Sigma w^{\frac{1}{2}}|F_o| = 0.105$, with a corresponding unweighted R of 0.108. The weighting scheme is $w = 9.79/[\sigma^2(F_o) + 0.000\,17(F_o)^2]$. Atomic co-ordinates are given in Table 2, and Table 3 contains bond lengths and angles. Structure factors and thermal parameters are contained in Supplementary Publication No. SUP 22726 (22 pp.).* Computations were made using the SHELX program [13] on the University of Cambridge's IBM 370/165. Neutral-atom scattering factors were taken from

TABLE 3

Bond lengths (Å) and angles (°) with estimated standard deviations in parentheses

(*a*) Lengths

O(1)–Fe(1)	2.213(7)	C(1)–C(2)	1.363(16)
O(2)–Fe(1)	2.194(7)	C(3)–C(4)	1.378(17)
N(1)–Fe(1)	2.100(9)	C(5)–C(6)	1.376(15)
N(2)–Fe(1)	2.242(8)	C(7)–C(8)	1.340(19)
N(4)–Fe(1)	2.126(7)	C(8)–C(9)	1.364(17)
N(5)–Fe(1)	2.112(8)	C(9)–C(10)	1.401(17)
N(7)–Fe(1)	2.276(8)	C(11)–C(10)	1.490(14)
C(10)–N(1)	1.324(15)	C(12)–C(1)	1.422(14)
C(17)–N(1)	1.351(13)	C(2)–C(18)	1.390(15)
C(11)–N(2)	1.270(14)	C(18)–C(3)	1.412(16)
N(2)–N(3)	1.393(11)	C(4)–C(19)	1.444(15)
C(23)–N(3)	1.491(16)	C(19)–C(5)	1.421(15)
N(3)–C(12)	1.395(14)	C(6)–C(15)	1.406(16)
N(4)–C(13)	1.353(13)	C(17)–C(7)	1.400(16)
N(4)–C(12)	1.306(13)	C(22)–C(11)	1.531(16)
N(5)–C(14)	1.340(12)	C(13)–C(14)	1.403(13)
N(5)–C(15)	1.327(13)	C(13)–C(18)	1.414(13)
C(15)–N(6)	1.418(13)	C(14)–C(19)	1.395(15)
C(20)–N(6)	1.474(16)	C(21)–C(16)	1.514(14)
N(6)–N(7)	1.359(13)	C(16)–C(17)	1.461(15)
N(7)–C(16)	1.290(13)	F(5)–B(2)	1.555(26)
F(1)–B(1)	1.338(15)	F(5′)–B(2)	1.385(28)
F(2)–B(1)	1.291(26)	F(6)–B(2)	1.480(27)
F(2′)–B(1)	1.459(26)	F(6′)–B(2)	1.248(29)
F(3)–B(1)	1.381(17)	F(7)–B(2)	1.327(26)
F(4)–B(1)	1.368(25)	F(7′)–B(2)	1.406(27)
F(4′)–B(1)	1.355(23)	F(8)–B(2)	1.347(24)
		F(8′)–B(2)	1.313(24)

TABLE 3 (*Continued*)

(*b*) Angles

O(2)–Fe(1)–O(1)	177.6(3)	C(9)–C(10)–N(1)	121.6(9)
N(1)–Fe(1)–O(1)	90.1(3)	C(11)–C(10)–N(1)	115.8(9)
N(1)–Fe(1)–O(2)	90.6(3)	C(11)–C(10)–C(9)	122.6(10)
N(2)–Fe(1)–O(1)	90.3(3)	C(8)–C(9)–C(10)	116.9(12)
N(2)–Fe(1)–O(2)	92.1(3)	C(7)–C(8)–C(9)	122.1(12)
N(2)–Fe(1)–N(1)	72.8(3)	C(17)–C(7)–C(8)	119.4(11)
N(2)–Fe(1)–N(4)	70.1(3)	C(7)–C(17)–N(1)	119.0(10)
N(2)–Fe(1)–N(5)	145.1(3)	C(16)–C(17)–N(1)	115.6(9)
N(2)–Fe(1)–N(7)	145.1(3)	C(16)–C(17)–C(7)	125.3(9)
N(4)–Fe(1)–O(1)	89.0(3)	C(21)–C(16)–C(17)	119.2(9)
N(4)–Fe(1)–O(2)	91.8(3)	N(7)–C(16)–C(17)	114.5(9)
N(4)–Fe(1)–N(1)	142.9(3)	N(7)–C(16)–C(21)	126.1(10)
N(4)–Fe(1)–N(7)	144.8(3)	C(6)–C(15)–N(6)	123.0(9)
N(4)–Fe(1)–N(5)	75.0(3)	N(5)–C(15)–N(6)	115.6(9)
N(5)–Fe(1)–O(1)	89.5(3)	N(5)–C(15)–C(6)	121.3(9)
N(5)–Fe(1)–O(2)	88.6(3)	C(5)–C(6)–C(15)	119.7(10)
N(5)–Fe(1)–N(1)	142.1(3)	C(19)–C(5)–C(6)	119.3(11)
N(5)–Fe(1)–N(7)	69.8(3)	C(14)–C(19)–C(5)	116.2(9)
N(7)–Fe(1)–O(1)	89.2(3)	C(4)–C(19)–C(5)	124.7(11)
N(7)–Fe(1)–O(2)	88.9(3)	C(4)–C(19)–C(14)	119.0(10)
N(7)–Fe(1)–N(1)	72.3(3)	N(5)–C(14)–C(19)	124.1(9)
C(10)–N(1)–Fe(1)	119.3(6)	C(13)–C(14)–C(19)	119.5(8)
C(17)–N(1)–Fe(1)	119.7(7)	C(13)–C(14)–N(5)	116.5(9)
C(17)–N(1)–C(10)	121.0(9)	H(4)–C(4)–C(19)	120.2(12)
N(3)–N(2)–Fe(1)	117.4(6)	C(3)–C(4)–C(19)	119.7(11)
C(11)–N(2)–Fe(1)	117.1(7)	C(18)–C(3)–C(4)	122.6(10)
C(11)–N(2)–N(3)	124.2(8)	C(13)–C(18)–C(3)	116.4(9)
C(23)–N(3)–C(12)	120.8(9)	C(2)–C(18)–C(3)	126.9(10)
N(2)–N(3)–C(12)	112.9(8)	C(2)–C(18)–C(13)	116.7(9)
N(2)–N(3)–C(23)	117.8(8)	C(18)–C(13)–C(14)	122.8(9)
C(13)–N(4)–Fe(1)	116.4(6)	N(4)–C(13)–C(14)	115.3(8)
C(12)–N(4)–Fe(1)	123.7(7)	N(4)–C(13)–C(18)	121.8(9)
C(12)–N(4)–C(13)	120.0(8)	C(1)–C(2)–C(18)	121.6(9)
C(15)–N(5)–Fe(1)	123.8(7)	C(12)–C(1)–C(2)	117.6(10)
C(14)–N(5)–Fe(1)	116.8(6)	N(4)–C(12)–C(1)	122.3(9)
C(14)–N(5)–C(15)	119.1(9)	N(3)–C(12)–C(1)	121.7(9)
C(20)–N(6)–N(7)	120.9(9)	N(3)–C(12)–N(4)	115.9(8)
C(15)–N(6)–N(7)	112.6(8)	N(2)–C(11)–C(10)	113.5(9)
C(15)–N(6)–C(20)	118.0(9)	C(22)–C(11)–C(10)	118.8(9)
C(16)–N(7)–Fe(1)	116.0(7)	C(22)–C(11)–N(2)	127.5(9)
N(6)–N(7)–Fe(1)	118.1(6)	F(6)–B(2)–F(5)	88.4(14)
N(6)–N(7)–C(16)	124.6(8)	F(7)–B(2)–F(5)	92.1(16)
F(2)–B(1)–F(1)	111.2(14)	F(6)–B(2)–F(7)	104.5(15)
F(3)–B(1)–F(1)	110.2(11)	F(8)–B(2)–F(5)	98.9(15)
F(3)–B(1)–F(2)	116.6(15)	F(8)–B(2)–F(7)	115.4(17)
F(4)–B(1)–F(1)	100.8(13)	F(8)–B(2)–F(6)	139.0(19)
F(4)–B(1)–F(2)	119.6(16)	F(5′)–B(2)–F(6′)	124.0(18)
F(4)–B(1)–F(3)	96.7(13)	F(7′)–B(2)–F(5′)	104.9(17)
F(4′)–B(1)–F(2′)	100.0(14)	F(7′)–B(2)–F(6′)	102.9(17)
		F(8′)–B(2)–F(5′)	106.0(17)
		F(8′)–B(2)–F(6′)	100.3(18)
		F(8′)–B(2)–F(7′)	120.1(16)

* For details see Notices to Authors No. 7, *J.C.S. Dalton*, 1979, Index issue.

ref. 14, with those for Fe, O, and N corrected for both parts of anomalous dispersion. The exponential series for a spherical, bonded hydrogen atom came from ref.15.

Discussion of the Structure.—The crystal structure of $[Fe(L^3)(OH_2)_2][BF_4]_2$ is illustrated in Figure 1, along with the numbering scheme adopted: hydrogen atoms and the anions have been omitted for clarity. The co-ordination geometry of the iron is approximately pentagonal bipyramidal with water molecules in the axial sites and the Fe atom seated in the macrocyclic cavity. The N_5 donor set of atoms, which form the pentagon, are coplanar (maximum deviation from the least-squares plane is 0.02 Å) and the axial oxygen donors are perpendicular to this plane. The macrocycle is roughly planar; the greatest displacement of any C or N atom from the N_5 plane, excluding the methyl carbons, is 0.30 Å. However, the plane of the phenanthroline group makes an angle of 4.2° with the N_5 plane. Details of these least-squares planes and of deviations of selected atoms from them are contained in Table 4. Interatomic separations indicate that the BF_4^- anions are unco-ordinated.

The Fe–N bond lengths lie within the range 2.10—2.28 Å and fall into two sets; Fe–N(heterocyclic), average length 2.11(2) Å, and Fe–N(hydrazone), 2.26(2) Å. Distances for a series of high-spin iron(II) complexes with more saturated quinquedentate macrocycles occur within the limits 2.16—2.29,[16] 2.22—2.26,[17] and 2.23—2.37 Å,[16] while the mean Fe–N length for the complex with 2,6-diacetylpyridinebis(semicarbazone) is 2.22 Å.[18] Iron–nitrogen bond lengths found in high-spin iron(II) porphyrin complexes are 2.086(4),[8] 2.072(5),[19] 2.069(15),[20] and 2.055(10) Å.[21] Angles subtended at the metal ion in $[Fe(L^3)(OH_2)_2][BF_4]_2$ by adjacent nitrogen donors fall in the range 69—75°, with the two lower values along with the longer Fe–N(hydrazone) bonds reflecting the rigidity of the macrocycle. Strain in the ring system is evident in the deviation of the angles N(3)–C(12)–N(4), 116(1)°, and N(5)–C(15)–N(6), 116(1)°, from the expected value of 120°. The average Fe–O bond length of 2.20(1) Å is similar to that found, 2.218(7) Å, in the high-spin pentagonal-bipyramidal iron(II) complex of another quinquedentate macrocycle.[17]

TABLE 4

Equations of least-squares planes,* with selected individual atomic deviations (Å) shown in square brackets

Plane 1: N(1), N(2), N(4), N(5), N(7)

$$11.58x + 2.77y + 7.86z = 9.93$$

[Fe −0.015(1), O(1) 2.199(3), O(2) −2.207(3), N(1) −0.002(3), N(2) −0.009(3), N(4) 0.016(3), N(5) −0.017(3), N(7) 0.011(3)]

Plane 2: Fe, N(1), N(2), N(4), N(5), N(7)

$$11.58x + 2.77y + 7.86z = 9.93$$

[Fe −0.012(1), O(1) 2.201(3), O(2) −2.205(4), N(1) 0.001(4), N(2) −0.006(3), N(4) 0.019(4), N(5) −0.015(4), N(7) 0.014(3)]

Plane 3: Pyridine ring

$$11.95x + 3.62y + 6.35z = 10.15$$

[Fe −0.041(2), N(4) −0.331(5), N(5) 0.085(3)]

Plane 4: Phenanthroline rings

$$12.11x + 2.27y + 7.08z = 10.06$$

[Fe 0.106(2), N(1) 0.271(4)]

Interplanar angles (°)

2	3	4	Plane
0.1	6.8	4.2	1
	6.8	4.2	2
		7.3	3

* x, y, and z are fractional atomic co-ordinates.

Comparison of bond lengths and angles with those measured in $[Mn(L^3)Cl][BF_4]$ shows only small differences between the two macrocycles.[1] However, the shapes of the ligands differ; L^3 is domed in the manganese(II) complex whereas here the macrocycle is approximately planar. One result of this variation is the different arrangements of the methyl groups in the two compounds. The short intramolecular contacts between C(20) and C(21), and C(22) and C(23), 3.02 and 2.99 Å respectively, are well inside the sum of their van der Waals radii, 4.0 Å.[22] The distances would be less but for partial relief of the interactions by axial displacement of the methyl groups. The difference between the iron(II) and manganese(II) complexes arises in the direction of these displacements. For the manganese(II) compound the hydrazine methyl carbons, C(20) and C(23), are on one side of the ring and the hydrazone methyl groups, C(21) and C(22), on the other side. The current iron(II) complex has a staggered arrangement of these groups: diagonally opposite Me groups are above the same face of the ligand while adjacent methyls are arrayed on opposite sides of the macrocycle. The average displacement of 0.67(1) Å is noticeably greater than the figure of 0.60(2) Å in $[Mn(L^3)Cl][BF_4]$. The increased tetrahedral distortion is also revealed in the sum of the bond angles at N(3) and N(6), 351.5° and 351.6° [358.9° and 354.9° in the manganese(II) derivative].

The remarkable feature of the crystal structure is that the seven-co-ordinate high-spin iron(II) is coplanar with the donor atoms of L^3. In the series of complexes $[M(L^3)]^{2+}$ (M = Fe, Zn, Mn, or Cd) where the metal ions are given in order of increasing radius,[23] it is only the smallest, high-spin Fe^{II}, that sits in the ligand plane. Chemical evidence indicates that the other cations have pentagonal-pyramidal co-ordination geometries, and by analogy with $[Mn(L^3)Cl][BF_4]$, the crystal structure of which is known,[1,2] these metal ions are displaced from the equatorial planes. A chloro-ligand occupies the axial site and L^3 forms the pentagon in these complexes. The coplanar co-ordination of Fe^{II} with L^3, despite the presence of chloride ions during the formation of the complex, strongly suggests that the co-ordination environment is determined by the relative radii of the cations and the cavity of L^3.

A diagram of the molecular packing, viewed along the crystallographic b axis is shown in Figure 2. The complex ions are separated by van der Waals distances. Hydrogen bonding between the BF_4^- ions and the water molecules is possibly present but the severe disorder of the anions prevents valid interatomic separations from being obtained.

Electrochemistry of the Macrocyclic Complexes.—The formation of the complexes $[M^{II}(L)]^{2+}$ (M = Fe, Mn, Zn, Cd, or Hg for L = L^2 or L^3 and M = Mn or Zn for L = L^4 or L^5) has been described in this paper and earlier

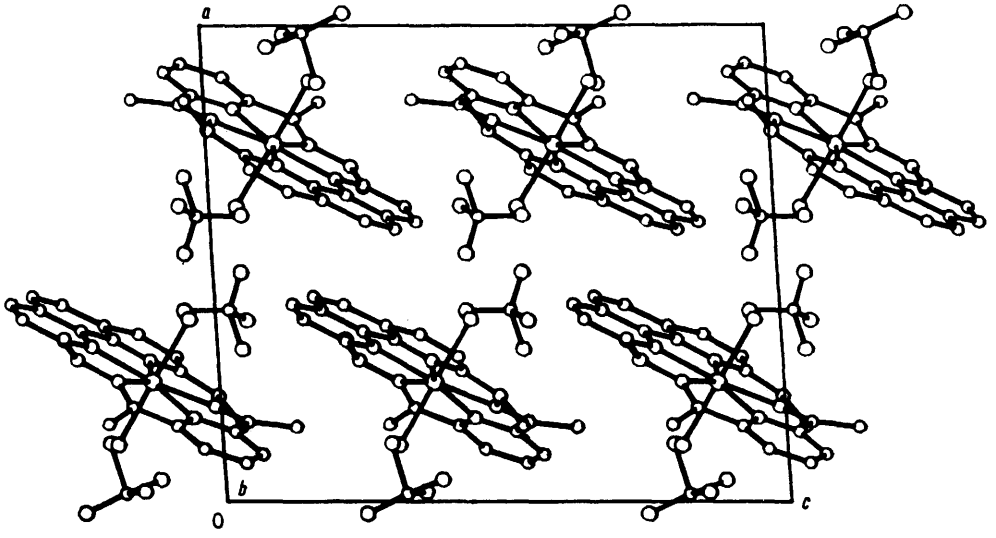

FIGURE 2 Molecular packing diagram of $[Fe(L^3)(OH_2)_2][BF_4]_2$. The unit cell is viewed along the *b* axis

members of the series.[1,2] In view of the interest in the electrochemical properties of macrocyclic complexes [5,24,25] the electrochemistry of several of the above compounds

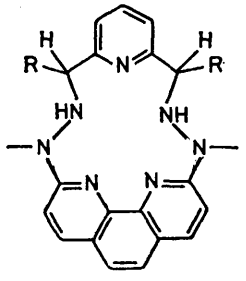

L^4: R = H
L^5: R = Me

was investigated. The techniques used were cyclic voltammetry and a.c. polarography, and the solvent for all measurements was dimethyl sulphoxide (dmso).

of the metal ion present. With the zinc(II) complex this wave has $\Delta E_p = 58$ mV; a reversible one-electron process.[26] Further proof of the reversibility is provided by the a.c. polarogram, where the wave has a half-peak width of 92 mV at an a.c. frequency of 61 Hz. The theoretical value for a reversible one-electron transfer is 93 mV.[27] The rarity of zinc(I) species and the almost constant reduction potential for different metal ions indicate that it is the ligand rather than the metal ion that is reduced, giving a π-anion radical. The corresponding wave in the voltammogram of the iron(II) complex is also reversible, $\Delta E_p = 64$ mV, while this electron transfer shows a small departure from reversibility for $[Mn(L^2)Cl][ClO_4]$ as $\Delta E_p = 76$ mV (23 °C, sweep rate 0.1 V s^{-1}). The analogous process with $Cd(L^3)Cl_2$ is irreversible. Voltammograms of the complexes exhibit a second reduction wave in the region −1.4 to −1.6 V. This wave appears to be quasireversible for the zinc(II) and iron(II) compounds but irreversible for the others. Comparison between the peak heights of the first and second waves suggest that this process is also a one-electron reduction. A chemical reaction follows this transfer as no return peaks were observed, and the anodic current for the first wave

TABLE 5

Cyclic voltammetry data for complexes of L^2 and L^3: potentials [a] of reduction waves

$[Mn(L^2)Cl][ClO_4]$		$[Fe(L^3)(OH_2)_2][BF_4]_2$		$[Zn(L^2)Cl][PF_6]$		$Cd(L^3)Cl_2$	
$E_{\frac{1}{2}}$	E_p	$E_{\frac{1}{2}}$	E_p	$E_{\frac{1}{2}}$	E_p	$E_{\frac{1}{2}}$	E_p
		0.24					
−1.106		−1.09		−1.04		−0.94 [b]	
						−1.19 [b]	
	−1.42		−1.49		−1.47	−1.58 [b]	
	−1.89		−2.04		−1.90		*c*

[a] Measured in volts relative to a Ag–AgCl electrode. [b] Values obtained from peak positions in the a.c. polarogram. [c] Several waves in this region.

Table 5 contains the potentials of the waves encountered, relative to a Ag–AgCl reference electrode. The complexes of L^2 and L^3 each give rise to at least three waves, one of which occurs close to −1.0 V irrespective

decreased if the voltage sweep went below −1.6 V. The wave at $E_{\frac{1}{2}} = 0.24$ V ($\Delta E_p = 70$ mV, scan rate 0.05 V s^{-1}) for $[Fe(L^3)(OH_2)_2][BF_4]_2$ is assigned to the Fe^{III}–Fe^{II} redox process. Voltammograms of complexes with the

reduced macrocycles L^4 and L^5 consist of a single reduction wave. For $[Zn(L^4)Cl][PF_6]$ the irreversible reduction has a peak potential of -1.70 V while $[Mn(L^5)Cl][BF_4]$ gives a quasireversible wave at $E_{\frac{1}{2}} = -1.66$ V ($\Delta E_p = 70$ mV, scan rate 0.2 V s^{-1}).

The variation in the first reduction potentials between complexes with L^2 and L^3 and those of L^4 and L^5 provides information relevant to the π delocalisation in the former ligands. This interpretation rests on the formation of a π-anion radical when $[ML^4]^{2+}$ or $[ML^5]^{2+}$ is reduced, a reasonable assumption considering that a less conjugated macrocycle than these ligands can stabilise the radical anion.[5] Altering the extent of conjugation will change the energy of the lowest-lying empty π orbital and hence the reduction potentials. Thus the movement of the first reduction wave from close to -1.0 V to approximately -1.7 V on passing between the two types of ligand signifies a change in the delocalisation present. As the only structural modification that has occurred is between the aromatic pyridine and phenanthroline units, the results indicate that the π systems extend completely around the macrocycles in L^2 and L^3.

EXPERIMENTAL

Infrared spectra were measured as Nujol mulls supported between sodium chloride discs, using Perkin-Elmer 257 and 457 spectrometers, over the range 625–4 000 cm^{-1}. A Newport variable-temperature Gouy balance provided the magnetic susceptibility data, with the readings corrected for ligand and inner-core diamagnetism by using Pascal's constants.[28] The Mössbauer spectrum was recorded on equipment described previously.[29] Microanalyses were performed by the University Chemical Laboratory Microanalytical Department.

Electrochemical measurements were recorded on a Princeton Applied Research Electrochemistry system, model 170. Ancillary equipment was either made on the premises or purchased from Metrohm. All readings were taken using a three-electrode potentiostatic system on 5×10^{-4} mol dm^{-3} solutions in dmso, with 10^{-1} mol dm^{-3} $[NBu^n_4][BF_4]$ present as the supporting electrolyte. A platinum wire sealed in glass served as the auxiliary electrode. Cyclic-voltammetry studies employed either a second platinum wire or a hanging-mercury-drop electrode (Metrohm). The dropping mercury electrode, for a.c. polarography, consisted of a six-inch long capillary down which triply-distilled mercury was allowed to pass. Constant drop times were provided by a P.A.R. drop timer. The Ag–AgCl reference electrode was made to a design kindly supplied by Heath and Hefter.[30] A salt bridge containing the solvent with the same concentration of base electrolyte as present in the bulk solution, was placed between the reference electrode and this solution.[31] The solvent was dried by distilling analytical grade dmso from calcium hydride, under reduced pressure. A published procedure was followed in the preparation and purification of the base electrolyte $[NBu^n_4][BF_4]$.[32] Deoxygenation of solutions was carried out by bubbling argon through the liquids.

Reagents, of analytical grade where possible, were used without further purification, apart from 2,6-diformylpyridine which was recrystallised from chloroform.

Iron(II) *Complexes of* L^2 *and* L^3.—The same general preparative method was followed for all the complexes, with the different anions being added after ring formation. The example given here is the synthesis of $[Fe(L^3)(OH_2)_2][BF_4]_2$. Fresh $FeCl_2 \cdot 4H_2O$ (0.14 g, 0.7 mmol) was added to water (75 cm^3) that had been refluxing in a stream of nitrogen for 10 min, and contained some ascorbic acid. This was followed by $L^1 \cdot HCl$ (0.7 mmol), and then 2,6-diacetylpyridine (0.7 mmol). The red colour of the solution turned to olive-green in the course of 0.5 h and the solution was kept refluxing for another 1 h. Addition of an excess of solid $Na[BF_4]$ and cooling gave olive-green platelets which were filtered off under nitrogen and dried *in vacuo*. Yield: 60%.

Support from the S.R.C. (to T. O' D., P. R. R., and J. N. R.) and from the British Council and the Association of Commonwealth Universities (to M. M. B.) is gratefully acknowledged. We thank Dr. S. Roquet-Covarrubias for running the Mössbauer spectrum, and Dr. G. Heath and Dr. G Hefter for advice on setting up the electrochemistry equipment.

[9/1033 *Received*, 2*nd July*, 1979]

REFERENCES

[1] Part 7, J. Lewis, T. D. O'Donoghue, and P. R. Raithby, preceding paper.
[2] M. M. Bishop, J. Lewis, T. D. O'Donoghue, and P. R. Raithby, *J.C.S. Chem. Comm.*, 1978, 476; Part 6, J. Lewis and T. D. O'Donoghue, *J.C.S. Dalton*, 1980, 743.
[3] M. D. Alexander, A. V. Heuvelen, and H. G. Hamilton, jun., *Inorg. Nuclear Chem. Letters*, 1970, **6**, 445.
[4] J. D. Curry and D. H. Busch, *J. Amer. Chem. Soc.*, 1964, **86**, 592.
[5] M. G. B. Drew, J. Grimshaw, P. D. A. McIlroy, and S. M. Nelson, *J.C.S. Dalton*, 1976, 1388.
[6] S. M. Nelson, S. G. McFall, M. G. B. Drew, A. H. Othman, and N. B. Mason, *J.C.S. Chem. Comm.*, 1977, 167.
[7] M. G. B. Drew, A. H. Othman, W. E. Hill, P. D. A. McIlroy, and S. M. Nelson, *Inorg. Chim. Acta*, 1975, **12**, L25.
[8] J. P. Collman, J. L. Hoard, N. Kim, G. Lang, and C. A. Reed, *J. Amer. Chem. Soc.*, 1975, **97**, 2676.
[9] G. B. Jameson, G. A. Rodley, W. T. Robinson, R. R. Gagne, C. A. Reed, and J. P. Collman, *Inorg. Chem.*, 1978, **17**, 850; L. J. Radonovich, A. Bloom, and J. L. Hoard, *J. Amer. Chem. Soc.*, 1972, **94**, 2073.
[10] M. M. Bishop, J. Lewis, T. D. O'Donoghue, P. R. Raithby, and J. N. Ramsden, *J.C.S. Chem. Comm.*, 1978, 828.
[11] K. Nakamoto, 'Infrared Spectra of Inorganic and Coordination Compounds,' 2nd edn., Wiley, New York, 1970.
[12] N. N. Greenwood and T. C. Gibb, 'Mössbauer Spectroscopy,' Chapman and Hall, London, 1971.
[13] G. M. Sheldrick, 'SHELX. A Crystallographic Computing Package,' Cambridge, 1976.
[14] 'International Tables for *X*-Ray Crystallography,' Kynoch Press, Birmingham, 1974, vol. 4.
[15] R. J. Stewart, E. R. Davidson, and W. J. Simpson, *J. Chem. Phys.*, 1965, **42**, 3175.
[16] M. G. B. Drew, A. H. Othman, and S. M. Nelson, *J.C.S. Dalton*, 1976, 1394.
[17] M. G. B. Drew, A. H. Othman, P. McIlroy, and S. M. Nelson, *Acta Cryst.*, 1976, **B32**, 1029.
[18] G. J. Palenik and D. W. Wester, *Inorg. Chem.*, 1978, **17**, 864.
[19] J. P. Collman, personal communication.
[20] G. B. Jameson, W. T. Robinson, J. P. Collman, and T. N. Sorrell, *Inorg. Chem.*, 1978, **17**, 858.
[21] P. Eisenberger, R. G. Schulman, B. M. Kincaid, G. S. Brown, and S. Ogawa, *Nature*, 1978, **274**, 30.
[22] L. Pauling, 'The Nature of the Chemical Bond,' 3rd edn., Cornell University Press, New York, 1960, p. 260.
[23] R. D. Shannon and C. T. Prewitt, *Acta Cryst.*, 1969, **B25**, 925.
[24] D. H. Busch, K. Farmery, V. Katovic, A. C. Melnyk, C. R, Sperati, and N. E. Tokel, *Adv. Chem. Ser.*, 1971, **100**, 44.
[25] F. V. Lovvechio, E. S. Gore, and D. H. Busch, *J. Amer.*

Chem. Soc., 1974, **96**, 3109; D. C. Olson and J. Vasilevskis, *Inorg. Chem.*, 1972, **11**, 980, and refs. therein.
[26] R. S. Nicholson and I. Shain, *Analyt. Chem.*, 1964, **36**, 704.
[27] A. M. Bond, *Analyt. Chem.*, 1972, **44**, 315.
[28] B. N. Figgis and J. Lewis, 'Modern Co-ordination Chemistry,' eds. J. Lewis and R. G. Wilkins, Interscience, New York, 1960.
[29] G. M. Bancroft, A. G. Maddock, and J. Ward, *Chem. and Ind.*, 1966, 423.
[30] G. Heath and G. Hefter, personal communication.
[31] J. N. Butler, *Adv. Electrochem. Electrochemical Engineering*, 1970, **7**, 77.
[32] H. O. House, E. Feng, and N. P. Peet, *J. Org. Chem.*, 1971, **36**, 2371.